Barker, P.F., Camerlenghi, A., Acton, G.D., and Ramsay, A.T.S. (Eds.)
Proceedings of the Ocean Drilling Program, Scientific Results Volume 178

11. Characteristics of Ice-Rafted Pebbles from the Continental Rise Sediment Drifts West of the Antarctic Peninsula (Sites 1095, 1096, and 1101)[1]

Lauren E. Hassler[2] and Ellen A. Cowan[2]

ABSTRACT

Pebbles (>10 mm) sampled from three drill sites on the continental rise west of the Antarctic Peninsula during Ocean Drilling Program Leg 178 were classified by shape and roundness. In addition, pebble lithology and surface texture were visually identified. To increase the pebble sample number to 331, three sites that were drilled 94 to 213 km from the continental shelf edge were integrated into the data set using magnetostratigraphy for core correlation. Pebbles were compared in three groups defined by the same stratigraphic intervals at each site: 3.1–2.2 Ma (late Pliocene), 2.2–0.76 Ma (late Pliocene-late Pleistocene), and 0.76 Ma to the Holocene. Pebble lithologies originate from sources on the Antarctic Peninsula margin. Most pebbles are metamorphic and sedimentary pebbles are rare (<6%), whereas mafic volcanic and intrusive igneous lithologies increase in abundance upsection.

Pebbles from 3.1 to 0.76 Ma, plotted on sphericity-roundness diagrams, indicate original transport as basal and supraglacial/englacial debris. Pebbles are abundant and of diverse lithology. From 0.76 Ma to the present, the number of pebbles is low and their shape characteristics indicate they originated as basal debris. Observed changes in ice-rafted pebbles can be explained by growth of an ice sheet and inundation of the Antarctic Peninsula topography by ice ~0.76 Ma. Prior to this, outlet and valley glaciers transported debris at high levels within and at the

[1]Hassler, L.E., and Cowan, E.A., 2001. Characteristics of ice-rafted pebbles from the continental rise sediment drifts west of the Antarctic Peninsula (Sites 1095, 1096, and 1101). *In* Barker, P.F., Camerlenghi, A., Acton, G.D., and Ramsay, A.T.S. (Eds.), *Proc. ODP, Sci. Results,* 178, 1–23 [Online]. Available from World Wide Web: <http://www-odp.tamu.edu/publications/178_SR/VOLUME/CHAPTERS/SR178_11.PDF>. [Cited YYYY-MM-DD]
[2]Department of Geology, Appalachian State University, Boone NC 28608, USA. Correspondence author: **cowanea@appstate.edu**

Initial receipt: 8 August 2000
Acceptance: 19 April 2001
Web publication: 25 July 2001
Ms 178SR-212

base of the ice. The mass accumulation rate of sand fluctuates and includes rounded quartz grains. Ice-sheet growth may have been accompanied by overall cooling from subpolar to polar glacial regimes, which halted meltwater production and enhanced the growth of ice shelves, which consequently reduced sediment supply to icebergs.

INTRODUCTION

A principal objective of Leg 178 was to compile a high-resolution history of grounded ice-volume fluctuations on the Pacific margin of the Antarctic Peninsula. The continental shelf contains the most direct information, but this record is incomplete and difficult to sample. A more complete but indirect record of Antarctic Peninsula glaciation is preserved in the hemipelagic sediment drifts on the continental rise. This study focuses on the shape, roundness, lithology, and surface texture of pebbles that were eroded and modified by glaciers on the Antarctic Peninsula and then transported offshore by icebergs. Originally, this study was designed to complement the calculation of the ice-rafted debris mass accumulation rate (IRD MAR) from Site 1101 (Cowan, **Chap. 10,** this volume) and included 81 pebbles >10 mm in diameter that were deposited since 3.1 Ma. Pebbles from Site 1101 were collected from the working half of the core during shipboard sampling. After preliminary analysis, pebbles from Sites 1095 and 1096, also on the continental rise, were obtained from the core repository to increase the sample size. The three sites are 500 km apart, parallel to the shelf, and range from 94 to 213 km from the continental shelf edge (Fig. **F1**). These proximal sites appear to share a similar distribution of IRD from Antarctic Peninsula glaciers since 3.1 Ma. The lithologies of 480 pebbles were identified in hand specimen and fine-grained lithologies were confirmed in thin section. Shape and roundness of 393 (undamaged) pebbles were measured. Of the 480 pebbles, 331 are from portions of the core that are younger than 3.1 Ma; of those, 318 were measured for shape and roundness.

METHODS

Clasts >1 cm were sampled from three drill sites (1101, 1095, and 1096) on the continental rise west of the Antarctic Peninsula during Leg 178 (Fig. **F1;** Table **T1**). In this study, each core was divided into three stratigraphic units based on the sediment characteristics at Site 1101 and using magnetostratigraphy for correlation between the three drill sites (Barker and Camerlenghi, 1999). Unit 1 (0–0.76 Ma), Unit 2 (0.76–2.2 Ma), and Unit 3 (2.2–3.1 Ma) have variable thicknesses at each site that depend on the linear sedimentation rate over the time period.

The lithology of each of the 331 pebbles was identified in hand specimen (Table **T1**). Thin sections were made for pebbles of fine-grained lithology. For simplicity, pebbles were also grouped as volcanic (felsic or mafic), intrusive, metamorphic, or sedimentary.

The long, intermediate, and short axes of each clast were measured using Vernier calipers. Sphericity was determined using Krumbein's (1941) intercept sphericity equation. Roundness was determined by comparing each dropstone to the Krumbein (1941) visual roundness chart. Shape was found using the Zingg (1935) shape diagram and assigning each pebble to a shape category of sphere, disc, blade, or rod.

F1. Location map for Sites 1101, 1095, and 1096, p. 8.

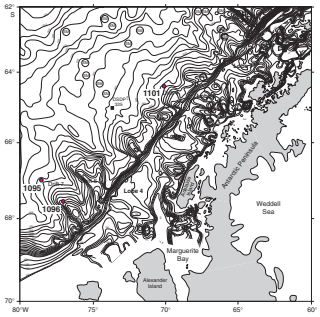

T1. Lithology, roundness, sphericity, shape, and surface texture of pebbles, p. 16.

Sphericity vs. roundness was plotted and contoured, then compared to similar plots by Boulton (1978) to determine in what zone within the glacier the pebbles were transported. Sixteen pebbles were damaged during drilling and were not included in analysis of roundness, sphericity, shape, and surface features.

RESULTS

Pebble abundance changes between each unit (Fig. F2). Unit 1 has the fewest pebbles (46) and fewest samples with >1 pebble (seen as peaks in Fig. F2). Unit 2, with the most pebbles (209), also has more peaks than any other unit. Unit 3 has fewer peaks than Units 1 and 2 but contains the largest peak (29 pebbles) of any unit.

Slight changes in lithology over time are present in the pebbles sampled for this study, which could indicate a change in sediment provenance. The percentage of metamorphic lithologies decreases with time from 62% to 41%, whereas intrusive lithologies increase from 8% to 20% (Fig. F3). There is a sharp increase (5% to 66%) in the number of mafic volcanic pebbles between Units 3 and 2, although there is no significant increase overall in volcanic clasts. The proportion of sedimentary lithologies remains consistently low throughout.

The relative abundance of each of the different clast shapes is constant through time, except for an increase in the proportion of rods from 9% to 19% (Fig. F4). Discs are the most common shape in all units, spheres are the next most common, but the proportions of blades and rods vary. Shapes of the pebbles appear to be controlled to some degree by their lithology. Discs are the most common shape for all lithologies, except intrusive igneous rocks (Fig. F5), for which spherical shapes are the most common. Rods are slightly more common than blades in volcanic and intrusive pebbles, whereas for metamorphic and especially sedimentary pebbles, blades are more common than rods.

Values of visual roundness are between 0.1 and 0.6 for Units 2 and 3 (Fig. F6). For Unit 1 the majority of pebbles have values of roundness between 0.3 and 0.5, with slightly fewer at 0.3 and no pebbles of value 0.1. Unit 1 has a higher percentage of pebbles with values of roundness of 0.3 than any other unit. In Unit 2, visual roundness values increase steadily from 0.1 to 0.5, then drop off sharply at 0.6. Unit 3 contains equal numbers of pebbles of values 0.4 and 0.5 and a significantly lower percentage of pebbles of value 0.3 than other units.

In all units, most pebbles fall within the field of basal debris on the sphericity vs. roundness diagram, as defined by Boulton (1978). In Unit 1, one pebble plots within the field for supraglacial debris. All others may be interpreted as basal debris (Fig. F7). All three fields, supraglacial, basal, and lodgement, are clearly represented in pebbles in both Units 2 and 3, although pebbles plotting in the supraglacial and lodgement fields are not as common in Unit 3 as in Unit 2.

DISCUSSION

The mode of transport within and the thermal regime of a glacier are thought to be important in determining pebble shape. Boulton (1978) examined pebbles from both temperate and polythermal glaciers and from different zones within glaciers. Fields for supraglacial/englacial, and basal debris, and lodgement till were defined by circumscribing the

F2. Frequency of pebbles vs. depth, p. 9.

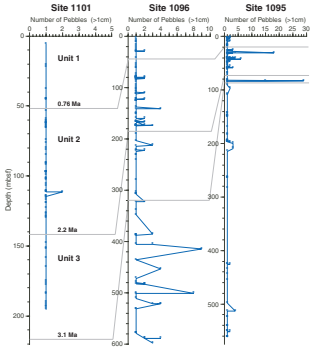

F3. Simplified lithology by percentage of pebbles by unit, p. 10.

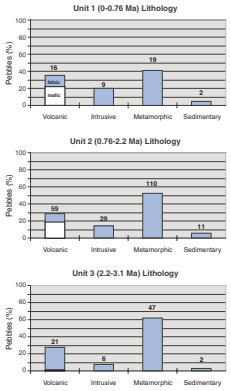

F4. Percentage of pebble shapes by unit, p. 11.

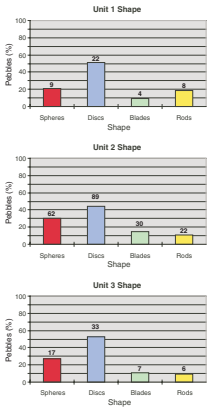

area in which 90% of the clasts in each category plotted on the sphericity vs. roundness graph. Boulton (1978) found that clasts that had fallen onto the glacier and were transported near the surface as supraglacial/englacial debris tend to retain their original shape and roundness because they are not subject to the abrasion and rotation that occurs at the bed of the glacier. Sphericity values for pebbles transported supraglacially are varied, but they are very angular, that is, they have low visual roundness (Boulton, 1978). Clasts eroded from the bed of the glacier and dragged along at the glacier sole (basal debris) tend to have distinctive surface features, intermediate roundness values, and slightly higher sphericity than supraglacial and englacial debris (Fig. F8). Clasts in the bed of the glacier that are deposited as lodgement till, not picked up and transported by the ice, tend to be abraded into faceted, more streamlined shapes with higher roundness values (Boulton, 1978).

Glacial thermal regime may also affect the shape of clasts (Hambrey, 1994; Kuhn et al., 1993). Kuhn et al. (1993) found that glaciers in very cold regions such as the Weddell Sea and the Lazarev Sea produce more angular clasts and cautioned against comparing temperate glaciers in the Northern Hemisphere with the extremely cold glaciers of Antarctica. Different climatic regimes influence the thermal characteristics of glaciers in a given region, which, in turn, may affect the amount of pebbles in each zone of transport (Hambrey, 1994). In the case of warm or temperate glaciers, meltwater flows to the bed of the glacier and facilitates sliding and erosion at the bed. The water also carries basal sediments away from the glacier. In the case of cold glaciers, if meltwater exists, it is surficial and usually seasonal (Hambrey, 1994). Movement is slower for the colder glacier, and there is less erosion of the bed. The basal layer of sediment, however, is thicker than that of the temperate glaciers (Hambrey, 1994). In Boulton's (1978) study, the Breidamerkurjökull in southeastern Iceland and the Søre Buchananisen in Spitsbergen correspond to the temperate and cold glaciers, respectively. Currently, the Antarctic Peninsula is warmer than the rest of the continent and has a moderate diversity of glacial types, including valley glaciers, glacier tongues, and outlet glaciers (Anderson et al., 1991). The northern Antarctic Peninsula is considered to be subpolar, whereas the rest of the continent is polar.

Icebergs calved from different types of glaciers may deposit sediments from each of the three zones of transport in different proportions (Domack et al., 1980). Ice sheets contribute small amounts of basal debris and only trace amounts of supraglacial/englacial debris (Hambrey, 1994). Basal debris is the first to be melted out of the ice when it enters the water; thus by the time icebergs calve from a large ice shelf, they may have very little sediment left (Anderson, 1999). Outlet and valley glaciers release a larger volume of sediment because they move faster and carry more debris, particularly supraglacial debris, than do ice sheets. These smaller glaciers carry a substantial amount of basal debris and varied amounts of supraglacial and englacial debris. However, their icebergs may not travel as far from the continent as large tabular icebergs from ice shelves.

The Antarctic Peninsula is the most likely source for dropstones found at Sites 1095, 1096, and 1101 based on the lithologies present and the proximity of the drill sites to the peninsula. The Scotia Arc region including the Antarctic Peninsula has a complex history of accretion and was an active plate margin both before and after the breakup of Gondwana (Barker et al., 1991). Greenschist to amphibolite facies

F5. Shape vs. lithology for all pebbles analyzed, p. 12.

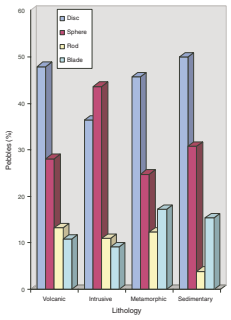

F6. Visual roundness of pebbles by unit, p. 13.

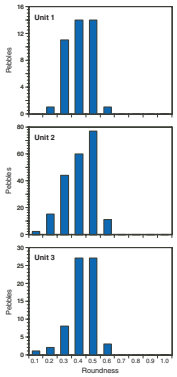

F7. Intercept sphericity and visual roundness of pebbles, p. 14.

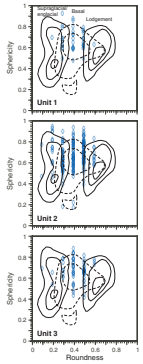

F8. Example of data from a basally transported pebble, p. 15.

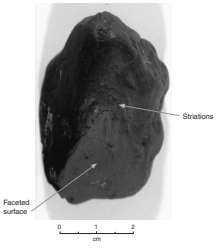

metasedimentary and metavolcanic rocks, including but not limited to deformed greywacke, conglomerate, greenschist, local blueschist, mafic lava, and undivided metasedimentary rocks on Alexander Island, represent a subduction complex accreted onto the peninsula before the breakup of Gondwana (Barker et al., 1991). Accreted forearc marine and volcaniclastic sedimentary units are also found on Alexander Island. Magmatic arc and subduction related lithologies such as calc-alkaline igneous rocks, rhyolite, andesite, and minor amounts of basalt and volcaniclastics are found on the peninsula (Barker et al., 1991). An increasing percentage of volcanic and calc-alkaline intrusive lithologies from Units 2 to 1, and a decreasing percentage of metamorphic lithologies, indicate a change in sediment provenance. The changes in lithology may reflect a lateral shift of source region, from the deformed accretionary prism (map Unit 3c; Barker et al., 1991), which now crops out extensively on Alexander Island, to younger intrusive complexes (map Units 9, 10a, 10b, and 17d), which now crop out on the peninsula, or a change in the level of erosion.

The overall shape of pebbles in our study has not changed significantly over the last 3 m.y. This probably reflects the fact that the major pebble lithologies identified in this study are fairly uniform over time. Foliated, bedded, or jointed rocks do not roll at the glacial bed as easily as massive rocks (Boulton, 1978); instead they tend to slide along the bed and form disc or blade shapes. Granite, granitic gneiss, and unfoliated volcanic tuffs tend to form rods and blades. Other lithologies tend to have foliation, bedding, or flow banding and are more likely to form flattened disc shapes. Metamorphic lithologies, particularly metavolcanics, were the most common rock type in each unit, which is reflected in the fact that discs are the dominant shape over time.

Sphericity and roundness of pebbles transported by icebergs to the continental rise sites over the last 3.0 m.y. show variability in the mode of glacial transport on the Antarctic Peninsula. There is a shift from a mixed population of pebbles representing transport in supraglacial, englacial, and basal debris zones within Unit 2 to a more restricted population that represents basal transport within Unit 1. Within Unit 2, pebbles are abundant and they represent diverse lithologies within mostly metamorphic and volcanic rock types. Within Unit 1, the total number of ice-rafted pebbles is smaller, as is the IRD MAR at Site 1101, based on the coarse sand fraction (Cowan, **Chap 10,** this volume). The lithology of pebbles is more restricted in Unit 1. There is an increase in the presence of basalt pebbles between Units 3 and 2, from 1.3% to 10.5%. The transition between Units 2 and 1 is present at 0.76 Ma and is marked by several other changes within the drift sediments. For example, at Site 1095 rounded quartz sand grains are absent from 0.78 to 0.2 Ma, even though the sand accumulation rate is similar in magnitude (Wolf-Welling et al., **Chap. 15,** this volume). At Site 1101, foraminifers are present within the interglacials until 0.76 Ma, after which they are replaced by diatoms (Barker, Camerlenghi, Acton, et al., 1999).

Often interpretations of ice-rafting records and pebble shape data are not clear cut and involve uncertainties (Anderson et al., 1980; Barrett, 1975, 1980; Domack et al., 1980; Kuhn et al., 1993). Several possibilities could account for the shift in the pebble population at the continental rise sites of this study: inundation of the continent by ice so that supraglacial debris is no longer available for transport; change in the glacial regime to more polar conditions, which would reduce the amount of debris and change the size and type of icebergs; long-term changes in iceberg drift tracks around the Antarctic Peninsula; and changes in oce-

anic conditions that would affect iceberg melting. Several of these conditions may have acted together to produce the shift in the observed variables. For example, rounded quartz sand grains may be produced by subglacial meltwater that is believed to have been more extensive under ice streams that advanced to the shelf edge in the past (Rebesco et al., 1998; Pudsey, 2000). The absence of rounded grains may indicate the absence of meltwater and colder glacial conditions between 0.78 and 0.2 Ma. Models of ice thickness during the late Wisconsinan maximum predict glacial ice up to 2000 m thick on the continental shelf near Marguerite Bay (Fig. **F1**) (Anderson et al., 1991). This thickness of ice, if extended inland over the continent, would be effective in inundating the topography and cutting off the supply of supraglacial debris from the mountain peaks and valley walls. Both thicker and colder ice would result in a reduced supply of debris available for rafting. Large tabular icebergs also survive greater transport distances and may bypass sites closer to the continent with their debris. We propose the hypothesis that climate conditions on the Antarctic Peninsula cooled and the ice sheet built up to great thickness sometime around 0.76 Ma, shortly after the mid-Pleistocene Climate Transition and the shift to 100-k.y. glacial–interglacial cyclicity (Cowan, **Chap. 10,** this volume). Although we favor topographic inundation and colder glacial conditions on the continent as the reason for the change in pebble population, we do acknowledge that oceanic changes have also occurred in the vicinity of the drift sites. Today, the Polar Front is close to the Antarctic Peninsula near Drift 4 and Site 1101 (Pudsey, 2000). It was probably closer to the continent between 2.2 and 0.76 Ma, when foraminifer-bearing mud was deposited during the interglacials at Site 1101. Because the pebble results at all three drift sites are similar and previous work in Antarctica did not yield systematic differences in the pebble shape between nearshore and distal sediments (Kuhn et al., 1993), we believe that oceanic influences on iceberg melt rates are not the major factor controlling the pebble shape variations at the drift sites.

ACKNOWLEDGMENTS

We wish to thank the shipboard scientific party of Leg 178 for initial sampling of dropstones from Site 1101 and also Walter Hale and Alex Wülbers at the Bremen Core Repository for sampling dropstones from Sites 1095 and 1096. This research was funded by a JOI-USSSP post-cruise research grant.

REFERENCES

Anderson, J.B., Domack, E.W., and Kurtz, D.D., 1980. Observation of sediment-laden icebergs in Antarctic waters: implications to glacial erosion and transport. *J. Glaciol.,* 25:387–396.

Anderson, J.B., Kennedy, D.S., Smith, M.J., and Domack, E.W., 1991. Sedimentary facies associated with Antarctica's floating ice masses. *In* Anderson, J.B., and Ashley, G.M., *Glacial marine sedimentation: Paleoclimatic significance,* GSA Special Paper 261:1–25.

Anderson, J.B., 1999. *Antarctic Marine Geology:* Cambridge (Cambridge Univ. Press).

Barker, P.F., and Camerlenghi, A., 1999. An approach to antarctic glacial history: the aims of Leg 178. *In* Barker, P.F., Camerlenghi, A., Acton, G.D., et al., *Proc. ODP, Init. Repts.,* 178, 1–44 [CD-ROM]. Available from: Ocean Drilling Program, Texas A&M University, College Station, TX 77845-9547, U.S.A.

Barker, P.F., Camerlenghi, A., Acton, G.D., et al., 1999. *Proc. ODP, Init. Repts.,* 178 [CD-ROM]. Available from: Ocean Drilling Program, Texas A&M University, College Station, TX 77845-9547, U.S.A.

Barker, P.F., Dalziel, I.W.D., and Storey, B.C., 1991. Tectonic development of the Scotia Arc region. *In* Tingey, R.J. (Ed.), *Geology of Antarctica:* Oxford (Oxford Univ. Press), 215–248.

Barrett, P.J., 1975. Characteristics of pebbles from Cenozoic marine glacial sediments in the Ross Sea (DSDP Sites 270–274) and the south Indian Ocean (Site 265). *In* Hayes, D.E., Frakes, L.A., et al., *Init. Repts. DSDP,* 28: Washington (U.S. Govt. Printing Office), 769–784.

Barrett, P.J., 1980. The shape of rock particles, a critical review. *Sedimentology,* 27:291–303.

Boulton, G.S., 1978. Boulder shapes and grain-size distribution of debris as indicators of transport paths through a glacier and till genesis. *Sedimentology,* 25:773–799.

Domack, E.W., Anderson, J.B., and Kurtz, D.D., 1980. Clast shape as an indicator of transport and depositional mechanisms in glacial marine sediments: George V Continental Shelf, Antarctica. *J. Sediment. Petrol.,* 50:813–820.

Hambrey, M., 1994. *Glacial Environments:* Vancouver (UBC Press).

Kirkbride, M.P., 1995. Processes of transportation. *In* Menzies, J. (Ed.), *Modern Glacial Environments:* London (Butterworth-Heinemann Ltd.), 9–76.

Krumbein, W.C., 1941. Measurement and geological significance of shape and roundness of sedimentary particles. *J. Sediment. Petrol.,* 11:64–72.

Kuhn, G. Melles, M., Ehrmann, W.V., Hambrey, M.J., and Schmiedl, G., 1993. Character of clasts in glaciomarine sediments as an indicator of transport and depositional processes, Weddell and Lazarev Seas, Antarctica. *J. Sediment. Petrol.,* 63:477–487.

Pudsey, C.J., 2000. Sedimentation on the continental rise west of the Antarctic Peninsula over the last three glacial cycles. *Mar. Geol.,* 167:313–338.

Rebesco, M., Camerlenghi, A., and Zanolla, C., 1998. Bathymetry and morphogenesis of the continental margin west of the Antarctic Peninsula. *Terra Antart.,* 5:715–728.

Zingg, T., 1935. Beitrage zur Schotteranalyse. *Schweiz. Miner. Petrog. Mitt.,* 15:38–140.

Figure F1. Location map for Leg 178 Sites 1101, 1095, and 1096 off the western margin of the Antarctic Peninsula (after Rebesco et al., 1998). SM = seamount. Four sediment lobes are found on the continental shelf between deep troughs.

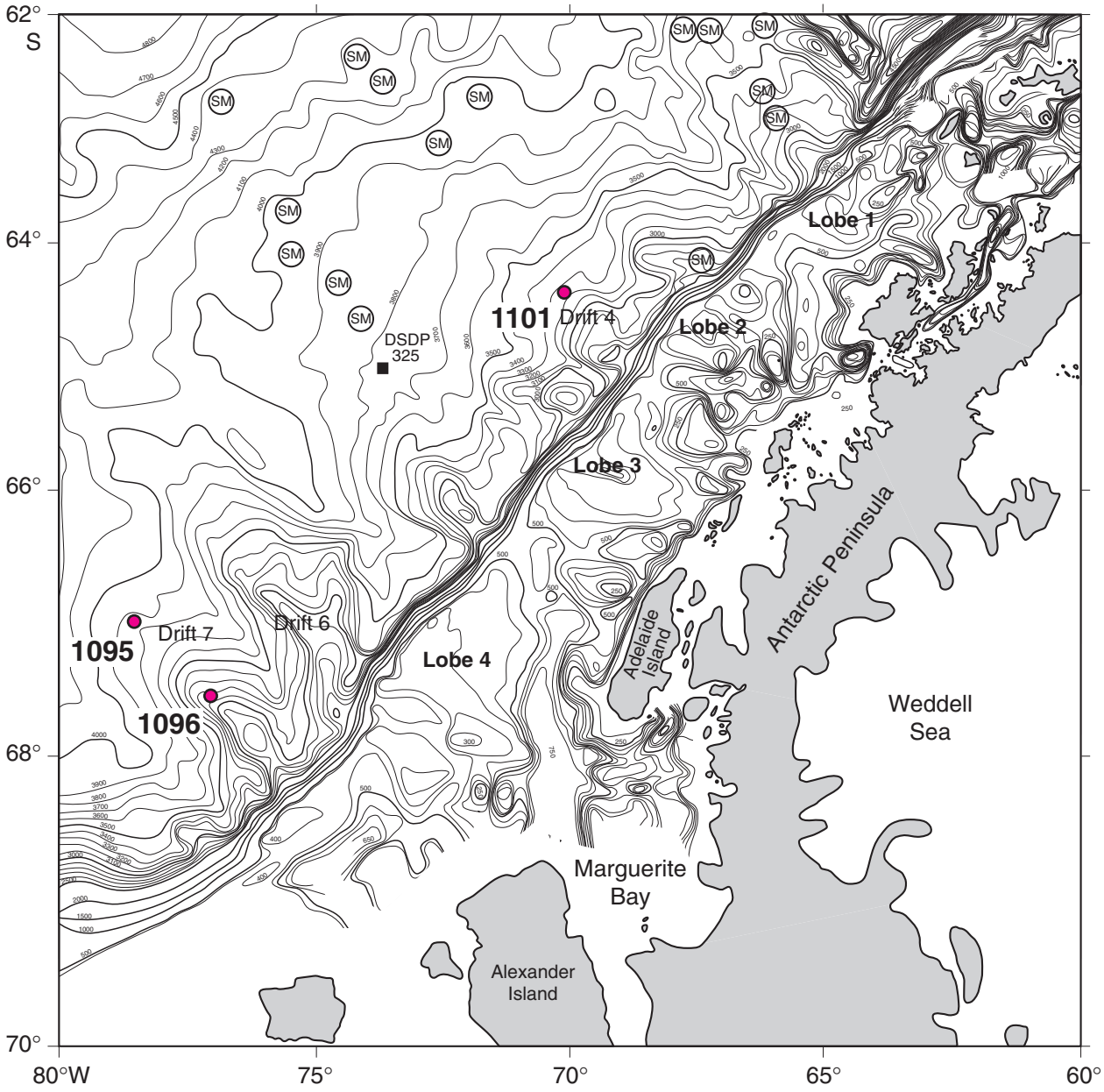

Figure F2. Frequency of pebbles (>1cm) vs. depth. Note the changes in depth scale between sites. Units are defined from Site 1101 and correlated to the other sites using linear sedimentation rates.

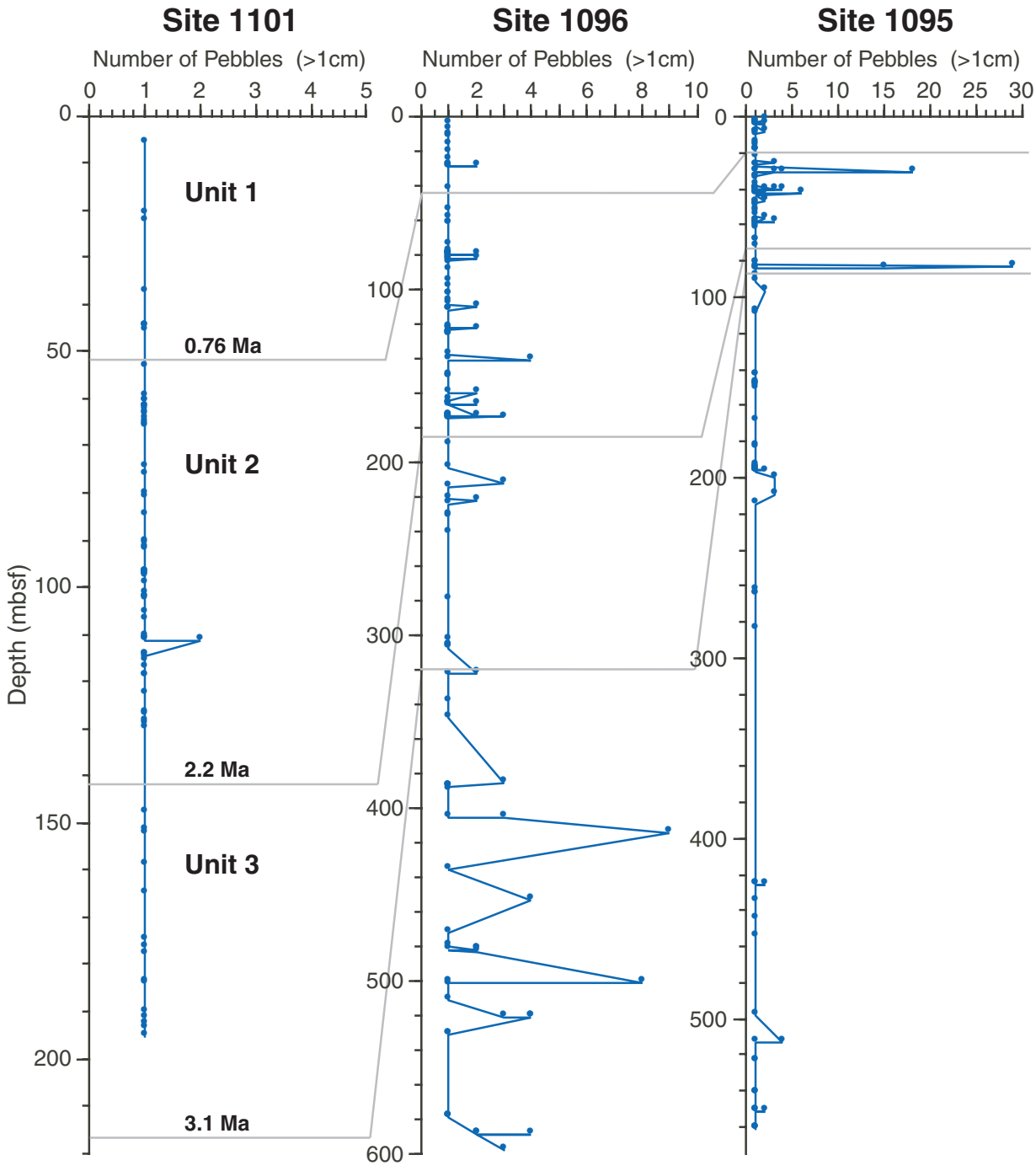

Figure F3. Simplified lithology by percentage of pebbles by unit. Numbers above columns indicate number of pebbles in each category. See Table T1, p. 16, for more detailed lithologic descriptions.

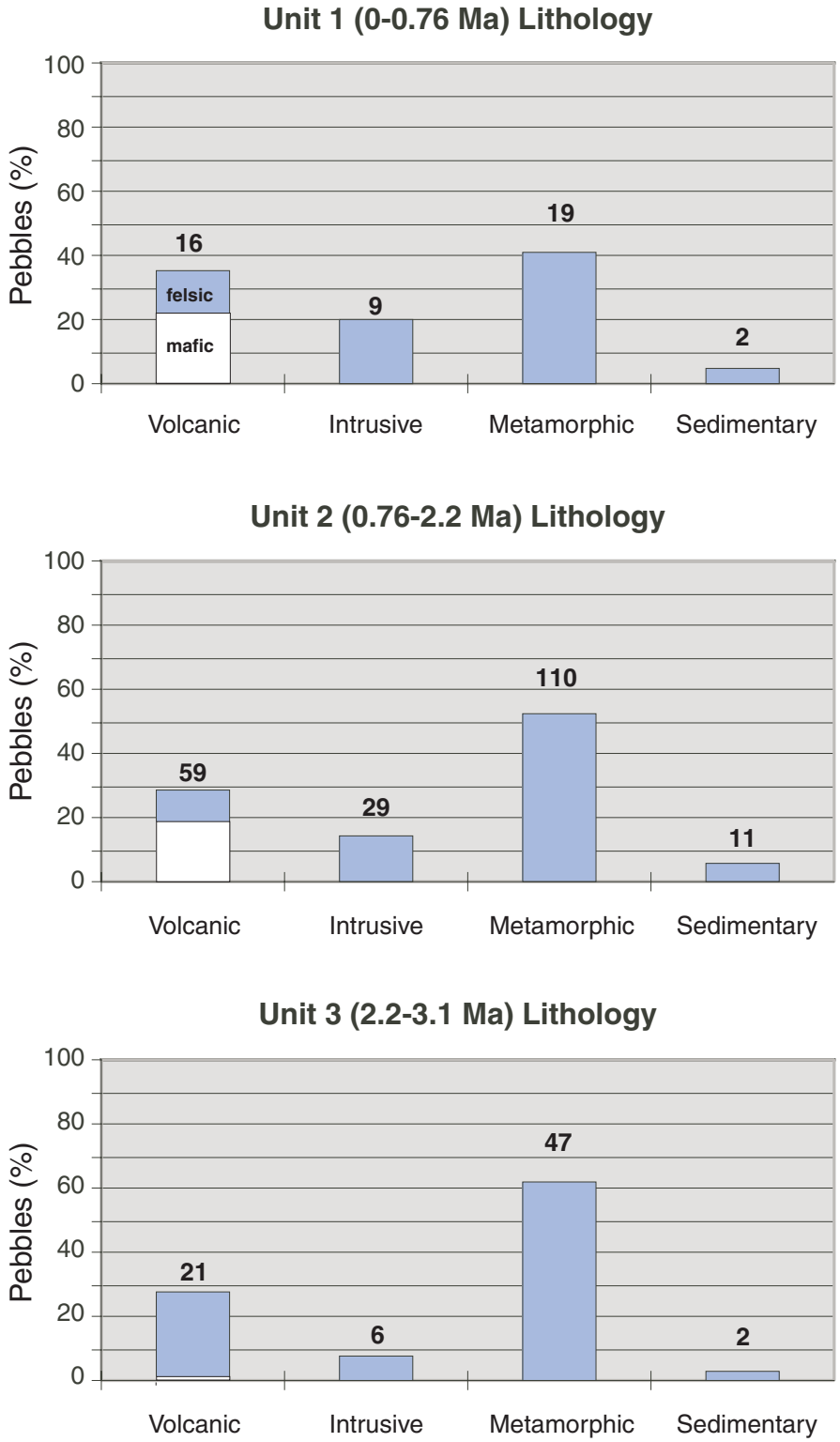

Figure F4. Percentage of pebble shapes by unit. The number of pebbles in each category is listed.

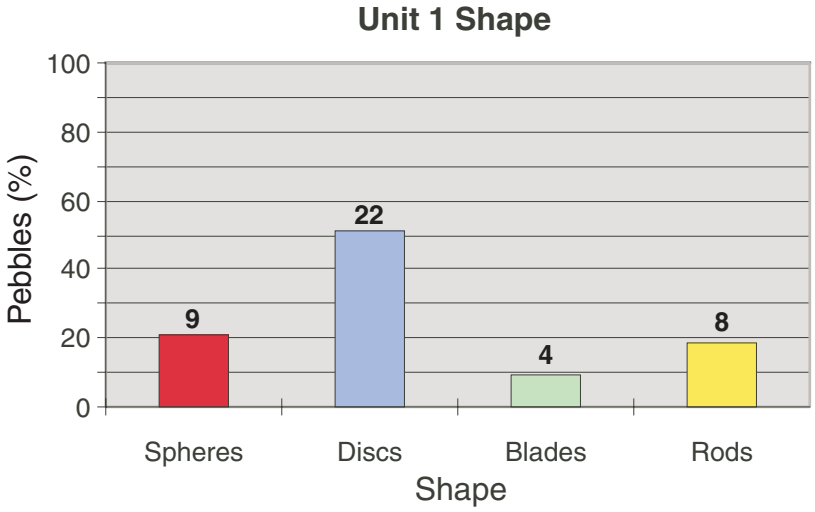

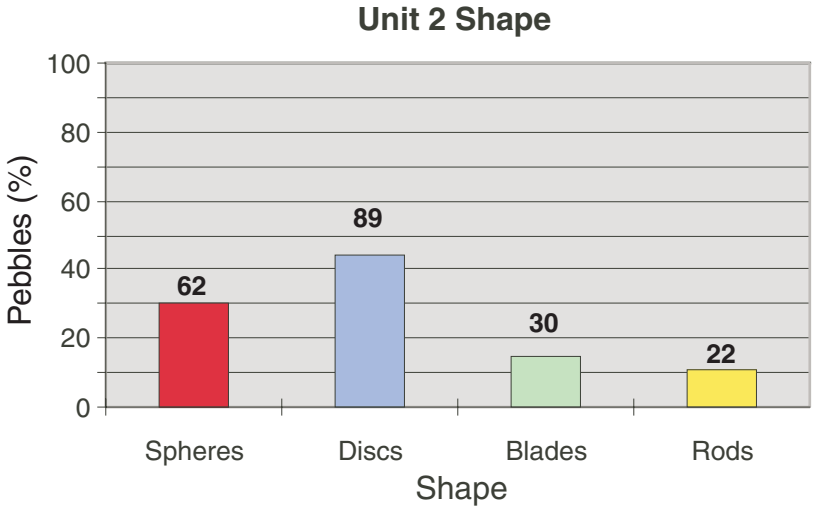

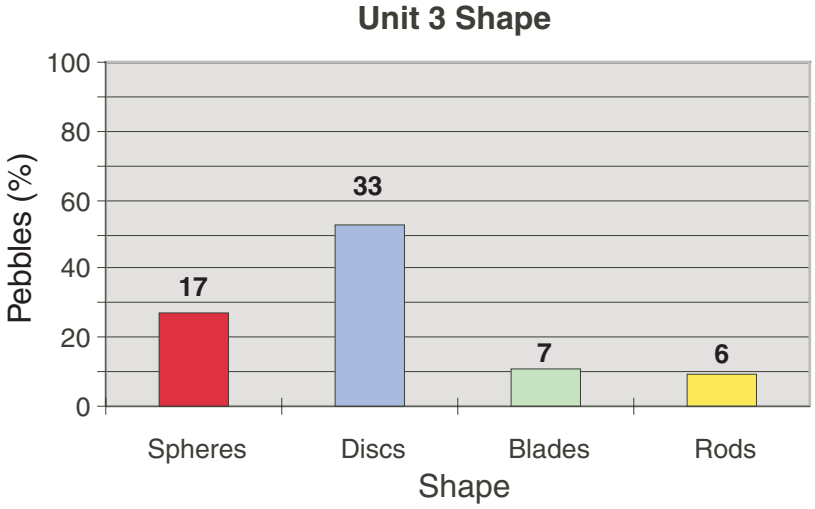

Figure F5. Shape vs. lithology for all pebbles analyzed.

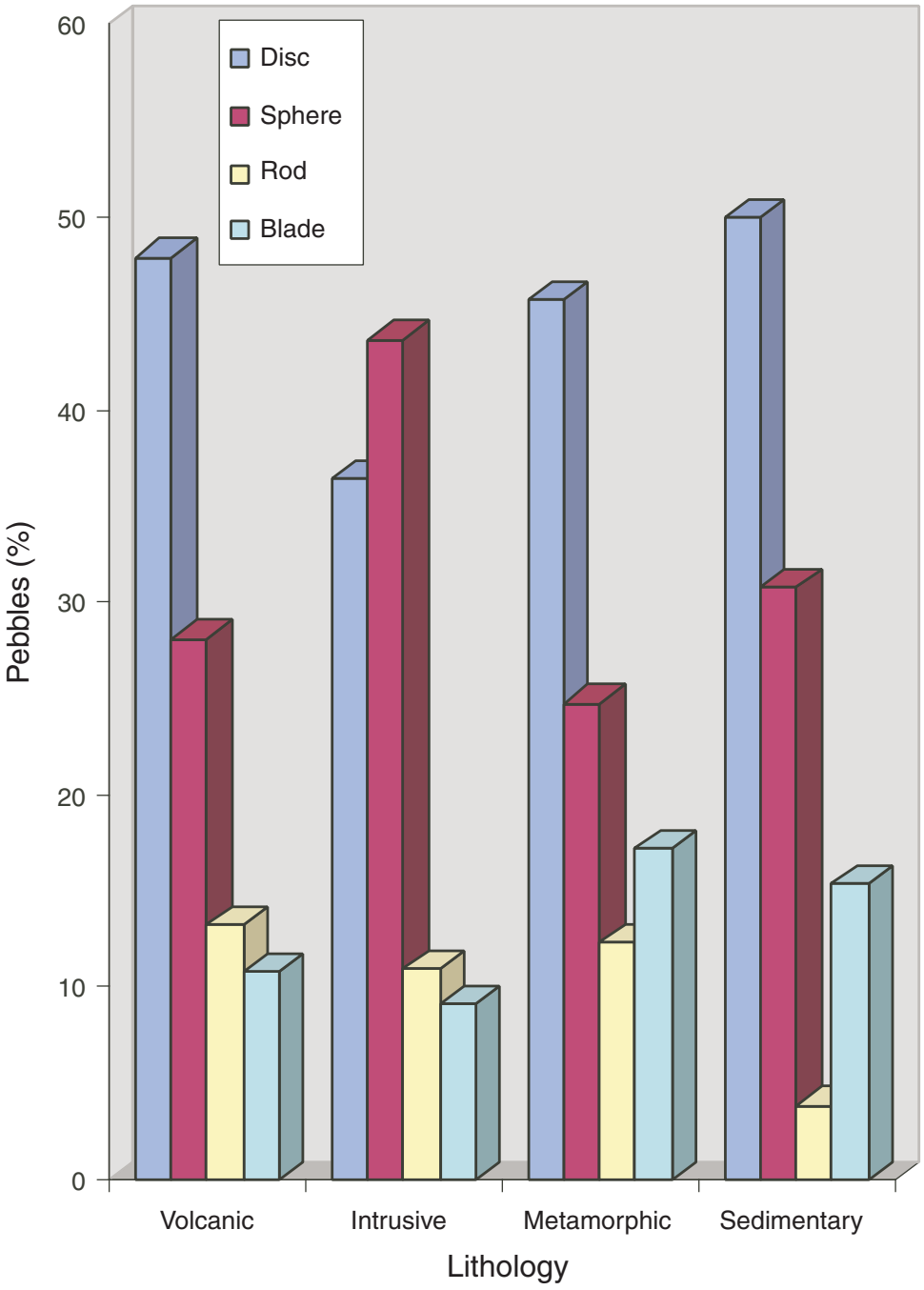

Figure F6. Visual roundness of pebbles by unit. Note the change in scale for the number of pebbles.

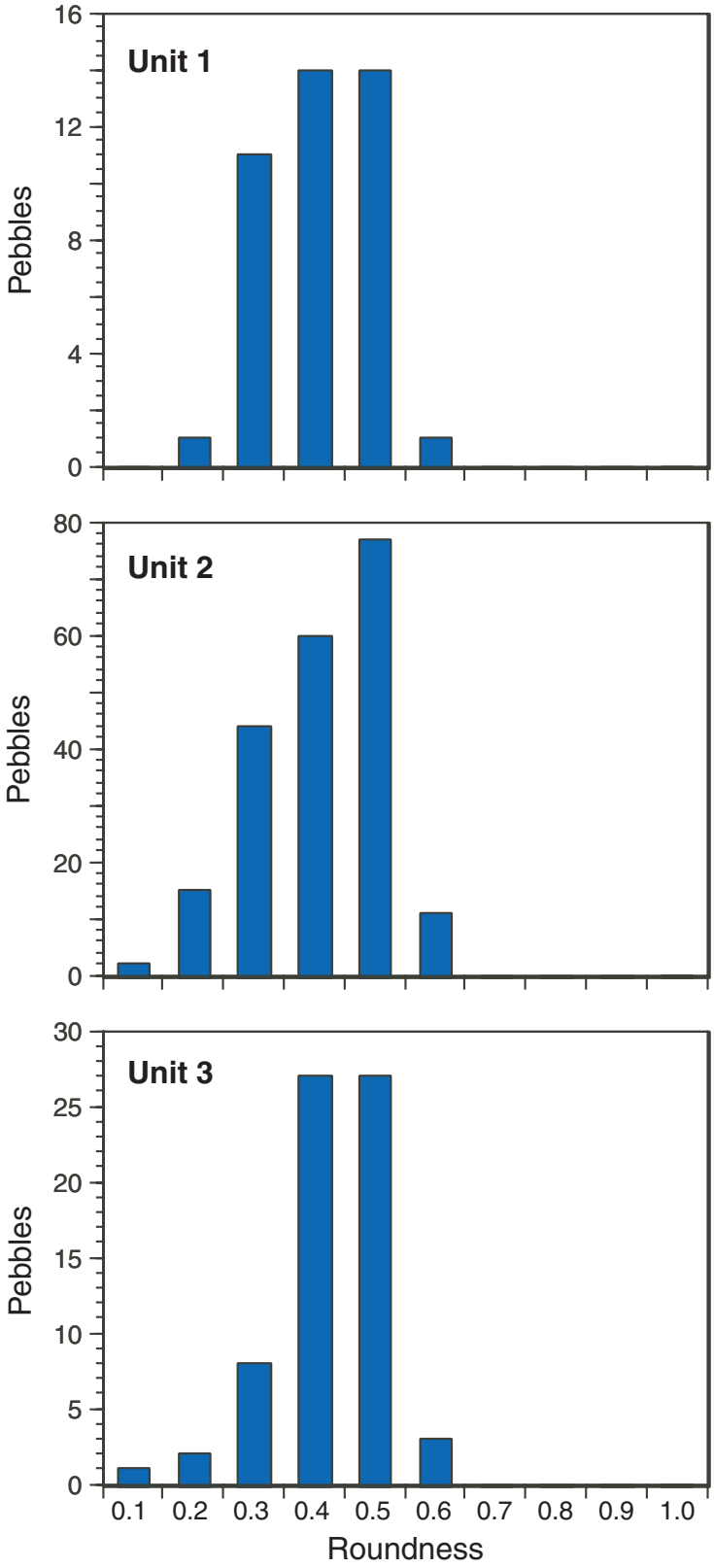

Figure F7. Intercept sphericity and visual roundness of pebbles plotted with zones of transport determined by Boulton (1978) for glacial clasts from Søre Buchananisen in Spitsbergen.

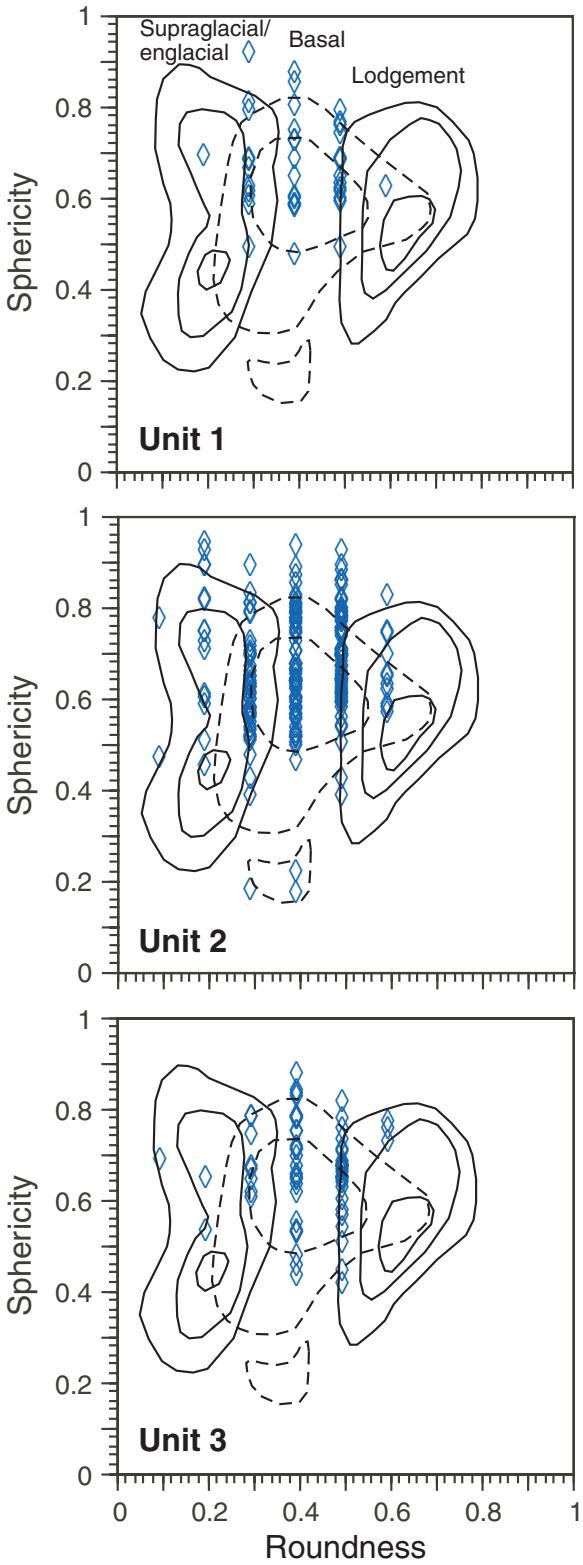

Figure F8. An example of data from a basally transported pebble from Site 1101. Roundness = 0.5, sphericity = 0.781, shape = rod, lithology = basalt.

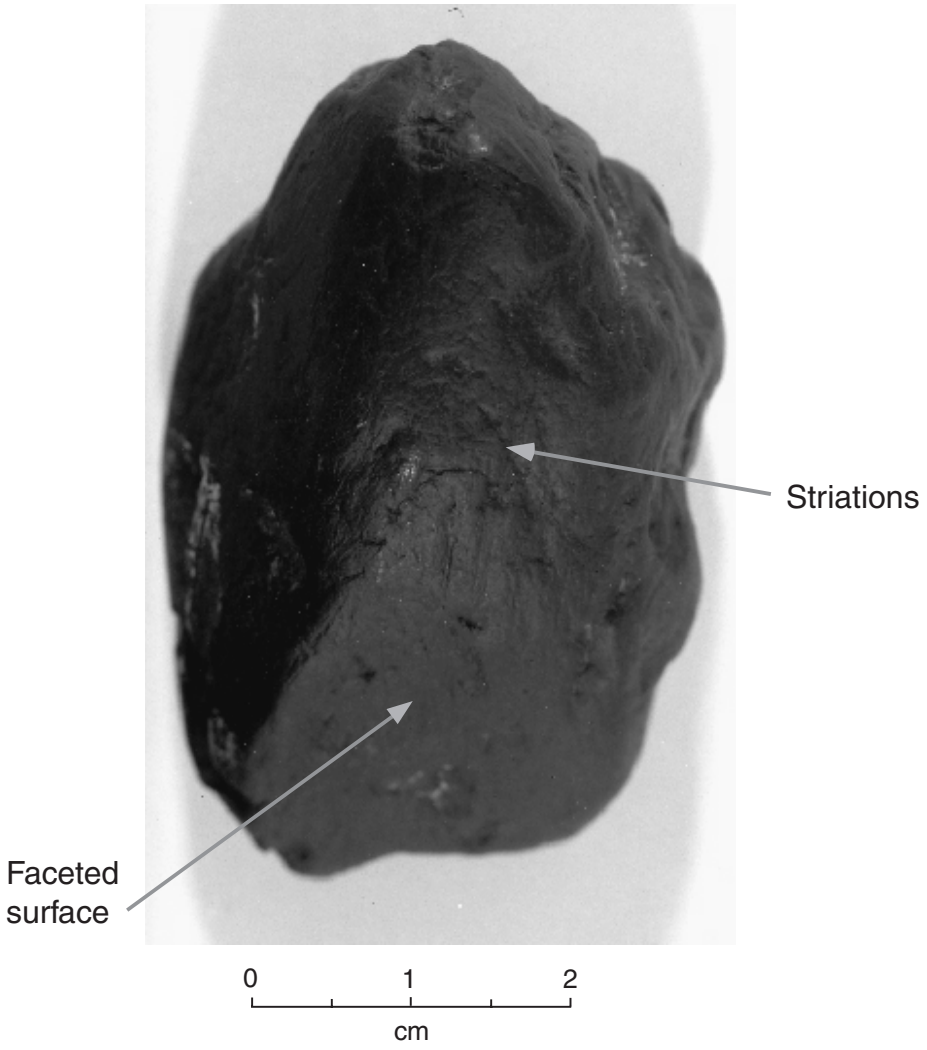

Table T1. Lithology, roundness, sphericity, shape, and surface texture of pebbles (>1 cm). (See table notes. Continued on next seven pages.)

Unit	Core, section, interval (cm)	Depth (mbsf)	Lithology	Roundness	Sphericity	Shape	Surface texture
1	178-1095A-						
	1H-2, 84a	2.30	Metavolcanic	0.4	0.713	Sphere	w
	1H-2, 84b	2.30	Granite	0.5	0.677	Disc	
	1H-3, 12	3.05	Diorite	0.6	0.614	Disc	
	1H-3, 49	3.42	Granite	0.3	0.705	Disc	
	1H-3, 91	3.84	Granite	0.4	0.864	Sphere	
	1H-3, 143	4.36	Basalt (scoria)				
	1H-4, 30	4.73	Andesite	0.3	0.482	Disc	w
	1H-4, 51	4.94	Metavolcanic	0.3	0.798	Sphere	w
	1H-4, 90	5.33	Andesite				
	2H-3, 105	9.95	Metavolcanic	0.3	0.605	Rod	
	2H-3, 12	9.02	Granite		0.772	Rod	
	2H-3, 34	9.24	Rhyolite	0.4	0.585	Disc	w
	3H-4, 25	15.15	Basalt	0.5	0.611	Disc	
	3H-4, 139	16.29	Lapilli tuff rhyolite	0.4	0.717	Sphere	s
2	4H-3, 36	24.16	Metavolcanic	0.5	0.661	Disc	s
	5H-1, 0a	30.30	Basalt	0.3	0.687	Sphere	w
	5H-1, 0b	30.30	Metarhyolite	0.4	0.587	Blade	w
	5H-1, 0c	30.30	Granite	0.4	0.626	Blade	
	5H-1, 0d	30.30	Metavolcanic	0.5	0.737	Rod	s
	5H-1, 0e	30.30	Metavolcanic	0.4	0.644	Disc	
	5H-1, 0f	30.30	Metavolcanic	0.4	0.509	Blade	
	5H-1, 0g	30.30	Metavolcanic	0.6	0.572	Blade	
	5H-1, 0h	30.30	Metavolcanic	0.6	0.797	Rod	w
	5H-1, 0i	30.30	Basalt	0.5	0.759	Sphere	
	5H-1, 0j	30.30	Basalt	0.6	0.607	Blade	
	5H-1, 0k	30.30	Rhyolite	0.5	0.916	Sphere	
	5H-1, 0l	30.30	Metavolcanic	0.5	0.629	Disc	
	5H-1, 0m	30.30	Metavolcanic	0.5	0.579	Disc	
	5H-1, 0n	30.30	Metavolcanic	0.5	0.417	Blade	s
	5H-1, 0o	30.30	Rhyolite	0.4	0.765	Sphere	
	5H-1, 0p	30.30	Mudstone	0.4	0.541	Disc	
	5H-1, 0r	30.30	Metarhyolite	0.2	0.497	Disc	w
	5H-1, 0s	30.30	Granite	0.4	0.84	Sphere	
	5H-1, 21a	30.51	Metavolcanic	0.4	0.616	Disc	
	5H-1, 21b	30.51	Metavolcanic	0.5	0.781	Sphere	
	5H-1, 21c	30.51	Granite	0.4	0.763	Rod	
	5H-1, 21d	30.51	Granite				
	5H-1, 24	30.54	Diorite	0.5	0.74	Sphere	w
	5H-1, 34	30.64	Basalt				
	5H-1, 55a	30.85	Metavolcanic	0.4	0.572	Blade	
	5H-1, 55b	30.85	Conglomerate	0.3	0.797	Sphere	
	5H-1, 55c	30.85	Quartz monzonite	0.3	0.466	Disc	s
	5H-3, 8	33.38	Rhyolite	0.4	0.456	Disc	w
	5H-3, 104	34.34	Metavolcanic	0.5	0.7	Sphere	
	5H-3, 115	34.45	Metarhyolite	0.4	0.795	Sphere	w
	5H-6, 1	37.81	Metabasalt	0.3	0.374	Disc	
	6H-1, 3a	39.83	Granite	0.4	0.651	Disc	
	6H-1, 3b	39.83	Metavolcanic	0.5	0.636	Disc	
	6H-1, 3c	39.83	Andesite	0.5	0.573	Disc	
	6H-1, 9	39.89	Gneiss	0.3	0.169	Disc	
	6H-1, 20	40.00	Schist				
	6H-1, 24a	40.04	Metavolcanic	0.5	0.604	Disc	
	6H-1, 24b	40.04	Metavolcanic	0.3	0.704	Sphere	
	6H-1, 24c	40.04	Metavolcanic	0.3	0.622	Blade	
	6H-1, 24d	40.04	Granite	0.5	0.731	Rod	s
	6H-1, 49a	40.29	Granite	0.4	0.876	Sphere	
	6H-1, 49b	40.29	Metavolcanic	0.5	0.839	Sphere	
	6H-1, 86	40.66	Quartzite	0.3	0.695	Sphere	w
	6H-1, 105	40.85	Metavolcanic	0.4	0.626	Disc	
	6H-1, 138a	41.18	Dacite	0.4	0.397	Disc	w
	6H-1, 138b	41.18	Sandstone	0.6	0.577	Disc	w
	6H-2, 57	41.87	Gneiss	0.4	0.566	Blade	w
	6H-2, 109	42.39	Amphibolite	0.5	0.532	Blade	
	6H-3, 25	43.05	Rhyolite	0.5	0.679	Disc	
	6H-3, 68	43.48	Rhyolite	0.5	0.699	Sphere	w
	6H-5, 82a	46.62	Metavolcanic				

Table T1 (continued).

Unit	Core, section, interval (cm)	Depth (mbsf)	Lithology	Roundness	Sphericity	Shape	Surface texture
	6H-5, 82b	46.62	Metavolcanic	0.5	0.641	Disc	
	6H-5, 113a	46.93	Metavolcanic	0.3	0.572	Disc	
	6H-5, 113b	46.93	Metavolcanic	0.5	0.687	Rod	
	6H-6, 134a	48.64	Rhyolite	0.4	0.554	Disc	
	6H-6, 17	47.47	Metavolcanic				
	7H-7, 36	58.66					
	7H-7, 53a	58.83	Andesite				
	7H-7, 53b	58.83	Metarhyolite	0.5	0.602	Disc	
	7H-7, 53c	58.83	Amphibolite				
	7H-7, 59	58.89	Metavolcanic				
	7H-7, 67	58.97	Basalt				
	8H-2, 66	60.96	Schist	0.5	0.68	Sphere	w
	8H-2, 108	61.38	Amphibolite				
	8H-3, 106	62.86	Rhyolite	0.3	0.558	Disc	w
	9H-3, 50	71.80	Andesite	0.5	0.66	Disc	
3	10H-3, 45	81.25	Metarhyolite	0.5	0.617	Disc	
	10H-3, 64	81.44	Andesite	0.3	0.736	Disc	w, s
3	178-1095B-						
	1H-1, 8a	83.08	Andesite				
	1H-1, 8aa	83.08	Metavolcanic	0.5	0.667	Rod	
	1H-1, 8b	83.08	Metavolcanic	0.5	0.568	Disc	s
	1H-1, 8bb	83.08	Granite	0.4	0.686	Disc	
	1H-1, 8c	83.08	Metavolcanic	0.5	0.672	Rod	
	1H-1, 8cc	83.08	Metasandstone	0.4	0.447	Blade	
	1H-1, 8d	83.08	Trachyte	0.5	0.768	Sphere	
	1H-1, 8dd	83.08	Metavolcanic	0.3	0.664	Disc	w
	1H-1, 8e	83.08	Metarhyolite	0.5	0.656	Disc	s
	1H-1, 8f	83.08	Metavolcanic	0.5	0.593	Disc	
	1H-1, 8g	83.08	Lapilli tuff rhyolite	0.4	0.666	Disc	w
	1H-1, 8h	83.08	Rhyolite	0.5	0.5	Disc	
	1H-1, 8i	83.08	Metarhyolite	0.5	0.557	Disc	
	1H-1, 8j	83.08	Metavolcanic	0.4	0.774	Sphere	
	1H-1, 8k	83.08	Rhyolite	0.4	0.775	Sphere	
	1H-1, 8l	83.08	Andesite	0.5	0.645	Disc	w
	1H-1, 8m	83.08	Rhyolite	0.3	0.776	Sphere	w
	1H-1, 8n	83.08	Metarhyolite	0.6	0.765	Sphere	w
	1H-1, 8o	83.08	Metarhyolite	0.6	0.749	Sphere	
	1H-1, 8p	83.08	Rhyolite	0.4	0.542	Blade	
	1H-1, 8q	83.08	Granite	0.4	0.704	Sphere	
	1H-1, 8r	83.08	Metavolcanic	0.5	0.699	Disc	
	1H-1, 8t	83.08	Metavolcanic	0.4	0.523	Disc	
	1H-1, 8u	83.08	Metavolcanic	0.4	0.521	Blade	
	1H-1, 8v	83.08	Granite	0.4	0.71	Disc	
	1H-1, 8w	83.08	Metavolcanic	0.5	0.409	Blade	
	1H-1, 8x	83.08	Andesite	0.4	0.623	Disc	w
	1H-1, 8y	83.08	Metavolcanic	0.5	0.436	Disc	
	1H-1, 8z	83.08	Metagranite	0.5	0.678	Disc	s
	1H-1, 68a	83.68	Metarhyolite	0.5	0.53	Disc	
	1H-1, 68b	83.68	Metavolcanic	0.5	0.64	Disc	
	1H-1, 68c	83.68	Rhyolite	0.4	0.872	Sphere	
	1H-1, 68d	83.68	Metavolcanic	0.5	0.666	Rod	w, s
	1H-1, 68e	83.68	Metavolcanic	0.4	0.424	Disc	
	1H-1, 68f	83.68	Metavolcanic	0.5	0.645	Disc	
	1H-1, 68g	83.68	Metasandstone	0.5	0.659	Disc	
	1H-1, 68h	83.68	Metavolcanic	0.4	0.772	Sphere	
	1H-1, 68i	83.68	Metarhyolite	0.4	0.649	Disc	s
	1H-1, 68k	83.68	Andesite	0.4	0.636	Disc	
	1H-1, 68l	83.68	Metavolcanic	0.5	0.727	Rod	
	1H-1, 68m	83.68	Metavolcanic	0.4	0.527	Blade	
	1H-1, 68n	83.68	Gneiss	0.6	0.72	Sphere	
	1H-1, 68o	83.68	Metarhyolite	0.5	0.75	Sphere	s
	1H-1, 68p	83.68	Rhyolite	0.4	0.74	Sphere	w
	1H-1, 101	84.01	Granite	0.4	0.818	Rod	
	1H-2, 2	84.52	Metasandstone	0.4	0.47	Blade	
	1H-2, 29	84.79	Metasandstone	0.4	0.642	Disc	
below 3	178-1095B-						
	1H-4, 39	not listed	Lithic wacke	0.3	0.754	Disc	
	1H-4, 54	not listed	Quartz monzonite				

Table T1 (continued).

Unit	Core, section, interval (cm)	Depth (mbsf)	Lithology	Roundness	Sphericity	Shape	Surface texture
	1H-5, 81	89.81	Rhyolite	0.5	0.725	Sphere	s
	1H-6, 117	91.67	Andesite	0.4	0.7	Disc	
	2H-2, 38	not listed	Metavolcanic				
	2H-3, 99a	96.49	Andesite	0.4	0.644	Disc	
	2H-3, 99b	96.49	Metavolcanic	0.5	0.777	Sphere	w
	2H-3, 111	not listed	Conglomerate				
	2H-4, 61	not listed	Andesite				
	2H-4, 79	not listed	Metavolcanic				
	3H-5, 117	109.17	Trachyte	0.3	0.657	Disc	
	3H-5, 20	108.20	Metarhyolite	0.5	0.704	Sphere	
	7H-3, 38	143.35	Granite	0.4	0.653	Disc	
	7H-3, 55	143.52	Gneiss	0.5	0.748	Sphere	
	7H-6, 48	147.95	Granite	0.3	0.456	Disc	
	7H-6, 125a	148.72	Basalt				
	7H-6, 125b	148.73	Metavolcanic				
	7H-6, 125c	148.74	Metavolcanic				
	8H-1, 66	150.16	Lapilli tuff rhyolite				
	8H-1, 143	150.93	Lithic wacke	0.5	0.669	Disc	
	10H-1, 13	168.63	Gneiss	0.5	0.537	Disc	
	11H-4, 127	183.77	Andesite	0.3	0.593	Disc	
	11H-4, 30	182.80	Andesite	0.4	0.756	Rod	
	12H-4, 121	193.21	Granite	0.2	0.682	Rod	
	12H-6, 13	195.13	Sandstone	0.3	0.456	Disc	
	12H-6, 23	195.23	Sandstone	0.3	0.536	Disc	
	12H-6, 39	195.39	Sandstone	0.2	0.407	Disc	
	12H-6, 54	195.54	Sandstone	0.3	0.529	Disc	
	12H-6, 117	196.17	Sandstone	0.3	0.358	Disc	
	12H-6, 127a	196.27	Sandstone	0.4	0.591	Blade	
	12H-6, 127b	196.27	Sandstone	0.3	0.595	Blade	
	12H-6, 132	196.32	Metavolcanic	0.5	0.505	Disc	
	12H-6, 139	196.39	Sandstone				
	12H-7, 3	196.53	Sandstone				
	12H-7, 11	196.61	Sandstone				
	13H-3, 109a	200.01	Granodiorite				
	13H-3, 109b	200.01	Granodiorite	0.2	0.832	Blade	w
	13H-3, 109c	200.01	Granodiorite	0.2	0.83	Rod	w
	14X-4, 46a	209.91	Metarhyolite	0.5	0.775	Rod	
	14X-4, 46b	209.91	Rhyolite	0.4	0.634	Disc	
	14X-4, 46c	209.91	Metavolcanic	0.3	0.585	Disc	
	15X-1, 38	215.08	Amphibolite	0.4	0.741	Sphere	
	20X-1, 60	263.30	Metavolcanic				
	20X-2, 87	265.07	Metavolcanic	0.3	0.716	Disc	w
	20X-2, 82	265.02	Metavolcanic	0.4	0.309	Disc	
	22X-2, 97	284.57	Granodiorite				
	37X-1, 1	425.81	Andesite?				
	37X-1, 8a	425.88	Quartz monzonite				
	37X-1, 8b	425.88	Quartz monzonite				
	37X-1, 12	425.92	Trachyte				
	38X-1, 0	435.50	Metavolcanic				
	39X-1, 0	445.10	Diamictite				
	40X-1, 0	454.80	Andesite				
	45X-1, 10	498.10	Metavolcanic	0.4	0.531	Blade	s
	47X-1, 0a	512.70	Granite				
	47X-1, 0b	512.70	Granite	0.3	0.777	Sphere	
	47X-1, 0c	512.70	Granite	0.4	0.748	Sphere	
	47X-1, 0d	512.70	Granodiorite	0.2	0.642	Disc	
	47X-1, 8	512.78	Granite				
	48X-1, 91	523.31	Siltstone				
	48X-1, 101	523.41	Basalt				
	50X-1, 1.5	541.72	Metavolcanic				
	50X-1, 7	541.77	Metarhyolite				
	50X-1, 10.5	541.80	Metavolcanic				
	51X-1, 0	551.40	Metavolcanic				
	51X-1, 4b	551.44	Basalt	0.2	0.625	Rod	
	51X-1, 4c	551.44	Basalt	0.2	0.401	Disc	
	51X-1, 8	551.48	Granite				
	51X-1, 11	551.51	Granite				
	52X-1, 0	560.80	Metavolcanic				
	52X-1, 1.5	560.82	Dacite				

Table T1 (continued).

Unit	Core, section, interval (cm)	Depth (mbsf)	Lithology	Roundness	Sphericity	Shape	Surface texture
	52X-1, 4	560.84	Andesite				
	52X-1, 48	561.28	Granite				
1	178-1095D-						
	1H-3, 81a	3.81	Basalt	0.3	0.612	Disc	w
	1H-3, 81b	3.81	Basalt	0.3	0.591	Disc	w
	2H-1, 0a	8.60	Basalt	0.4	0.576	Blade	w
	2H-1, 0b	8.60	Latite	0.3	0.672	Rod	w
	2H-1, 128	9.88	Basalt	0.5	0.747	Sphere	w
	2H-5, 130	15.90	Metavolcanic	0.5	0.48	Disc	
	3H-1, 32	18.42	Metavolcanic				
	3H-1, 45	18.55	Metavolcanic	0.4	0.79	Sphere	w
	3H-1, 59	18.69	Metavolcanic	0.5	0.67	Rod	
	3H-1, 66	18.76	Rhyolite	0.4	0.843	Sphere	
2	178-1095D-						
	3H-6, 33a	25.93	Metavolcanic	0.3	0.645	Disc	
	3H-6, 33b	25.93	Granite	0.5	0.742	Sphere	
	3H-6, 33d	25.93	Rhyolite	0.5	0.58	Blade	
	3H-6, 137	26.97	Rhyolite	0.3	0.817	Sphere	
	3H-6, 142	27.02	Metavolcanic				
	5H-2, 133	39.93	Metavolcanic	0.4	0.86	Sphere	
	5H-3, 40	40.50	Metabasalt	0.4	0.741	Sphere	
	5H-4, 59a	42.19	Metavolcanic	0.4	0.665	Disc	
	5H-4, 59b	42.19	Quartzite	0.3	0.565	Disc	
	5H-4, 80a	42.40	Metabasalt	0.3	0.525	Disc	
	5H-4, 80b	42.40	Rhyolite	0.4	0.776	Sphere	
	5H-4, 80d	42.40	Metavolcanic	0.5	0.848	Sphere	
	5H-4, 80e	42.40	Metavolcanic	0.4	0.502	Blade	
	5H-4, 80g	42.40	Metavolcanic	0.2	0.807	Sphere	
	5H-4, 80h	42.40	Metavolcanic	0.4	0.207	Blade	
	5H-4, 124	not listed	Quartz diorite	0.4	0.731	Sphere	
	6H-1, 93	47.53	Metavolcanic	0.4	0.755	Sphere	
	6H-3, 50	49.40	Metavolcanic	0.5	0.869	Sphere	w
	6H-3, 84	49.74	Basalt	0.5	0.591	Disc	
	6H-7, 7	52.28	Rhyolite	0.5	0.846	Sphere	w
	6H-7, 133a	53.54	Granite	0.3	0.554	Blade	
	6H-8, 114	54.85	Rhyolite				
	7H-1, 10a	56.20	Metavolcanic	0.4	0.502	Disc	
	7H-1, 10b	56.20	Rhyolite	0.3	0.602	Rod	
	7H-2, 94	58.54	Metavolcanic	0.3	0.688	Disc	
	8H-3, 43	69.03	Andesite	0.5	0.629	Disc	w
	8H-3, 78	69.38	Basalt	0.5	0.494	Disc	
1	178-1096A-						
	2H-3, 100	11.70	Metavolcanic	0.4	0.569	Disc	
	2H-3, 113	11.83	Rhyolite	0.5	0.732	Sphere	
	3H-1, 4	17.24	Andesite	0.4	0.638	Disc	
2	178-1096B-						
	6H-6, 145	54.65	Rhyolite	0.5	0.6	Blade	w
	7H-3, 111	59.31	Metavolcanic	0.5	0.627	Disc	w
	9H-1, 24.5	74.44	Gneiss	0.3	0.519	Disc	
	9H-5, 77	79.75	Metabasalt				
	9H-5, 126.5a	80.25	Metavolcanic	0.3	0.637	Disc	
	9H-5, 126.5b	80.25	Trachyte	0.4	0.619	Disc	
	9H-6, 16	80.64	Granite				
	9H-6, 22	80.70	Diorite				
	9H-6, 78	81.26	Metavolcanic				
	9H-7, 40	82.35	Andesite	0.4	0.631	Rod	
	11H-3, 1.5	96.21	Granite	0.5	0.744	Sphere	
	13H-1, 4	112.24	Basalt	0.5	0.618	Disc	s
	13H-1, 12	112.32	Metasandstone	0.6	0.643	Disc	
	13H-1, 63	112.83	Metavolcanic	0.4	0.809	Sphere	
	14H-1, 123	122.93	Metavolcanic	0.5	0.63	Disc	
	14H-1, 129a	122.99	Metavolcanic	0.5	0.584	Blade	s
	14H-1, 129b	122.99	Metavolcanic	0.3	0.587	Blade	
	14H-2, 8	123.28	Basalt	0.4	0.572	Disc	
	14H-2, 70	123.90	Gneiss	0.4	0.776	Sphere	
	14H-3, 64	125.34	Basalt	0.5	0.547	Blade	s
	14H-3, 106	125.76	Metabasalt	0.4	0.549	Disc	

Table T1 (continued).

Unit	Core, section, interval (cm)	Depth (mbsf)	Lithology	Roundness	Sphericity	Shape	Surface texture
	14H-3, 137	126.07	Biotite schist	0.4	0.662	Rod	
	14H-4, 10	126.30	Metavolcanic	0.5	0.768	Sphere	s
	14H-4, 20	126.40	Schist	0.3	0.498	Disc	
	14H-4, 66	126.86	Sandstone	0.2	0.737	Sphere	
	15H-CC, 2	138.37	Rhyolite	0.3	0.596	Disc	s
1	178-1096B-						
	2H-1, 82	4.62	Metasandstone	0.5	0.582	Blade	s
	2H-4, 9	8.39	Metavolcanic	0.4	0.463	Blade	w
	3H-6, 59	21.39	Metavolcanic	0.5	0.674	Disc	s
	4H-4, 11.5	26.07	Metavolcanic	0.4	0.739	Rod	
	4H-6, 4.5	29.00	Metavolcanic	0.5	0.621	Disc	
	4H-6, 40	29.35	Metasandstone	0.4	0.574	Disc	
	4H-6, 44a	29.39	Metasandstone	0.2	0.682	Disc	
	4H-6, 44b	29.39	Rhyolite	0.4	0.673	Disc	
	4H-6, 69	29.64	Metavolcanic	0.3	0.578	Disc	
	4H-6, 73	29.68	Metavolcanic	0.5	0.605	Disc	
	5H-7, 52.5	41.83	Granite				
2	178-1096B-						
	8H-2, 15	62.45	Metavolcanic	0.5	0.768	Sphere	
	8H-2, 4	62.34	Metavolcanic	0.5	0.696	Rod	
	10H-1, 52	80.32	Metavolcanic	0.5	0.851	Sphere	
	10H-1, 56.5	80.36	Sandstone	0.6	0.622	Blade	
	10H-1, 84	80.64	Metavolcanic	0.1	0.457	Blade	w
	10H-1, 112	80.92	Metavolcanic	0.3	0.502	Blade	
	10H-1, 139	81.19	Basalt	0.5	0.375	Blade	
	10H-2, 7	81.37	Basalt	0.4	0.624	Disc	
	10H-2, 55	81.85	Lithic arenite				
	10H-2, 115	82.46		0.2	0.804	Rod	
	10H-2, 115.5	82.46	Basalt				
	10H-3, 77.5	83.57	Metasandstone	0.3	0.661	Disc	w
	10H-3, 91	83.71	Quartzite	0.5	0.778	Rod	
	10H-4, 82	85.12	Metabasalt	0.4	0.796	Rod	
	10H-4, 110	85.40	Basalt	0.5	0.648	Rod	w
	11H-2, 31	91.11	Metabasalt	0.3	0.588	Blade	
	12H-1, 18	98.98	Andesite	0.4	0.523	Blade	
	12H-4, 50	103.80	Metavolcanic				
	12H-4, 58	103.88	Metagranite				
	13H-1, 71	109.01	Siltstone	0.5	0.772	Rod	s
	13H-1, 108	109.38	Metavolcanic	0.4	0.162	Disc	
	13H-1, 145a	109.75	Metasandstone	0.4	0.692	Disc	
	13H, 1, 145b	109.75	Basalt	0.5	0.683	Rod	s
	16H-4, 138a	141.08	Metavolcanic	0.5	0.691	Disc	
	16H-4, 138b	141.08	Metabasalt	0.2	0.913	Sphere	
	16H-4, 138c	141.08	Granite	0.3	0.613	Disc	
	16H-4, 138d	141.08	Rhyolite	0.4	0.738	Sphere	
	16H-5, 5	141.25	Granite				
	19H-1, 0	150.70	Diorite	0.5	0.758	Sphere	s
	19H-1, 8	150.78	Metavolcanic	0.4	0.628	Disc	
	19H-1, 26	150.96	Metavolcanic	0.4	0.653	Disc	w
	20H-2, 116	160.36	Metavolcanic	0.5	0.631	Disc	
	20H-2, 149a	160.69	Metavolcanic	0.5	0.671	Sphere	
	20H-2, 149b	160.69	Andesite	0.3	0.508	Disc	
	20H-5, 131.5	165.01	Metavolcanic				
	21H-1, 2b	not listed?	Metasandstone	0.3	0.612	Blade	
	22X-1, 1	166.91	Metavolcanic	0.5	0.736	Sphere	
	23X-1, 4	174.04	Basalt	0.5	0.811	Sphere	
	23X-1, 7	174.07	Basalt	0.6	0.636	Disc	w, s
	23X-1, 12a	174.12	Metavolcanic	0.4	0.608	Disc	w
	23X-1, 12b	174.12	Metarhyolite	0.6	0.559	Disc	w
	23X-1, 12c	174.12	Rhyolite	0.5	0.705	Disc	w
	22X-1, 23	167.13	Metavolcanic				
	23X-1, 51	174.51	Andesite	0.4	0.631	Disc	
	23X-1, 57	174.57	Andesite	0.4	0.514	Disc	
	23X-1, 121	175.21	Basalt	0.5	0.528	Blade	
	23X-2, 13	175.66	Gneiss	0.4	0.646	Disc	w
	23X-2, 33	175.86	Basalt				
3	24X-5, 57	190.08	Quartz monzonite				
	26X-1, 80	203.70	Metavolcanic				

Table T1 (continued).

Unit	Core, section, interval (cm)	Depth (mbsf)	Lithology	Roundness	Sphericity	Shape	Surface texture
	29X-1, 2a	231.72	Metavolcanic	0.3	0.661	Disc	w
	29X-1, 108	232.78	Metavolcanic				
	30X-1, 7	241.37	Metasandstone	0.5	0.663	Disc	
2	178-1096C-						
	2H-1, 6a	167.06	Metavolcanic	0.4	0.555	Blade	
	2H-1, 6b	167.06	Rhyolite	0.5	0.78	Sphere	
	2H-1, 18	167.18	Amphibolite	0.4	0.758	Sphere	
	2H-1, 45	167.45	Metavolcanic	0.5	0.684	Disc	
	2H-5, 43a	173.64	Quartz monzonite	0.4	0.692	Disc	
	2H-5, 43b	173.64	Metavolcanic	0.4	0.583	Disc	
	2H-5, 61	173.82	Andesite	0.3	0.502	Disc	
	2H-5, 75	173.96	Basalt	0.3	0.539	Disc	
	2H-5, 135	174.56	Metavolcanic	0.4	0.489	Disc	
	2H-6, 3	174.79	Metavolcanic	0.5	0.691	Disc	
3	5X-1, 49a	212.69	Metavolcanic				
	5X-1, 49b	212.69	Metavolcanic				
	5X-1, 49c	212.69	Metavolcanic				
	5X-2, 103	214.73	Metavolcanic				
	6X-1, 0	221.80	Metavolcanic	0.4	0.702	Disc	w
	6X-1, 29a	222.09	Metavolcanic				
	6X-1, 29b	222.09	Metavolcanic				
	6X-2, 135	224.65	Metavolcanic	0.3	0.636	Disc	
	10X-1, 64	280.64	Granite				
	12X-4, 87.5	303.30	Metavolcanic				
	12X-6, 114	306.57	Metavolcanic				
	12X-7, 18	307.11	Amphibolite				
	12X-7, 81	307.74	Metavolcanic				
	12X-7, 86.5	307.80	Metavolcanic				
below 3	14X-4, 11a	322.00	Metavolcanic	0.4	0.802	Sphere	
	14X-4, 11b	322.00	Basalt	0.4	0.568	Blade	
	14X-4, 110	322.99	Metavolcanic				
	16X-1, 103	338.93	Metavolcanic	0.5	0.727	Sphere	
	17X-1, 58	348.08	Metabasalt	0.5	0.73	Rod	
	21X-1, 0a	386.20	Granite	0.3	0.72	Sphere	w
	21X-1, 0b	386.20	Quartz monzonite				
	21X-1, 0c	386.20	Quartz monzonite				
	21X-3, 50	387.71	Andesite	0.5	0.748	Sphere	
	21X-3, 58	387.79	Andesite?				
	21X-3, 91	388.12	Metavolcanic				
	21X-3, 119	388.40	Metavolcanic				
	21X-4, 144	390.15	Basalt	0.4	0.413	Blade	
	23X-1, 0	405.50	Andesite				
	23X-1, 15a	405.65	Basalt				
	23X-1, 15b	405.65	Metavolcanic				
	23X-1, 15c	405.65	Metavolcanic				
	24X-1, 0a	415.10	Metavolcanic	0.5	0.604	Blade	s
	24X-1, 0b	415.10	Metavolcanic				
	24X-1, 0c	415.10	Metavolcanic	0.4	0.483	Disc	
	24X-1, 0d	415.10	Quartz monzonite	0.4	0.643	Disc	
	24X-1, 0e	415.10	Granite	0.4	0.789	Sphere	
	24X-1, 0f	415.10	Metavolcanic	0.4	0.576	Disc	
	24X-1, 0g	415.10	Metavolcanic	0.5	0.698	Sphere	
	24X-1, 0h	415.10	Amphibolite				
	24X-1, 0i	415.10	Amphibolite				
	26X-1, 111	435.51	Metavolcanic				
	28X-1, 0a	453.60	Andesite				
	28X-1, 0b	453.60	Granite				
	28X-1, 0c	453.60	Quartz monzontite				
	28X-1, 0d	453.60	Metavolcanic	0.3	0.372	Disc	
	30X-1, 0	472.90	Metavolcanic				
	30X-6, 0	480.40	Andesite				
	30X-CC, 6a	482.42	Granite	0.5	0.723	Sphere	
	30X-CC, 6b	482.42	Basalt	0.4	0.428	Disc	
	30X-CC, 12a	482.48	Granite				
	30X-CC, 12b	482.48	Amphibolite?				
	30X-CC, 15	not listed	Metavolcanic				
	30X-CC, 37	482.73	Granite	0.4	0.706	Disc	
	31X-1, 137a	483.87	Lithic arenite				

Table T1 (continued).

Unit	Core, section, interval (cm)	Depth (mbsf)	Lithology	Roundness	Sphericity	Shape	Surface texture
	31X-1, 137b	483.87	Metavolcanic				
	33X-1, 0a	501.70	Metavolcanic				
	33X-1, 0b	501.70	Quartz monzonite				
	33X-1, 0c	501.70	Metavolcanic	0.4	0.53	Disc	
	33X-1, 0c2	501.70	Metavolcanic				
	33X-1, 0d	501.70	Rhyolite				
	33X-1, 0e	501.70	Quartz monzonite	0.3	0.779	Sphere	
	33X-1, 0f	501.70	Andesite				
	33X-1, 0g	501.70	Basalt				
	33X-1, 11	501.81	Metavolcanic	0.5	0.544	Disc	w
	33X-1, 16	501.86	Metavolcanic				
	34X-1, 0	511.40	Metavolcanic				
	35X-1, 0a	521.00	Metabasalt	0.4	0.806	Sphere	
	35X-1, 0b	521.00	Metavolcanic	0.4	0.662	Disc	
	35X-1, 0c	521.00	Metavolcanic	0.4	0.55	Blade	
	35X-1, 5a	521.05	Metavolcanic				
	35X-1, 5b	521.05	Rhyolite				
	35X-1, 5c	521.05	Metasandstone	0.5	0.769	Sphere	
	35X-1, 5d	521.05	Metavolcanic	0.3	0.751	Sphere	
	35X-1, 8a	521.08	Metavolcanic				
	35X-1, 8b	521.08	Metavolcanic	0.5	0.622	Disc	w
	35X-1, 8c	521.08	Metavolcanic				
	35X-1, 8d	521.08	Metavolcanic	0.3	0.753	Sphere	
	36X-1, 11	530.81	Metavolcanic				
	36X-1, 15	530.85	Metavolcanic				
	41X-1, 0	579.10	Rhyolite				
	41X-1, 8	579.18	Granite				
	41X-1, 15	579.25	Metavolcanic				
	41X-1, 16	579.26	Quartz diorite	0.4	0.578	Disc	
	42X-1, 0a	588.60	Granite				
	42X-1, 0b	588.60	Basalt	0.5	0.855	Sphere	
	42X-1, 8a	588.68	Metavolcanic	0.6	0.671	Rod	
	42X-1, 8b	588.68	Granite				
	42X-1, 0c	588.68	Amphibolite				
	42X-1, 0d	588.68	Metavolcanic				
	42X-1, 13a	588.73	Metavolcanic	0.5	0.746	Sphere	
	42X-1, 13b	588.73	Granite	0.3	0.724	Sphere	
	43X-CC, 0a	598.10	Granodiorite	0.3	0.618	Blade	
	43X-CC, 0b	598.10	Metavolcanic	0.5	0.747	Rod	
	43X-CC, 0c	598.10	Metabasalt	0.5	0.633	Disc	
1	178-1101-						
	1H-4, 143	5.93	Metarhyolite	0.5	0.587	Blade	s, p
	3H-2, 122	20.92	Andesite	0.3	0.655	Rod	
	3H-3, 143	22.63	Metarhyolite	0.5	0.752	Rod	w, p
	5H-CC, 6	37.75	Diorite	0.4	0.592	Disc	w
	6H-5, 53	44.73	Granite	0.3	0.782	Sphere	
	6H-5, 70	44.90	Granite	0.3	0.674	Disc	
	6H-5, 93	45.13	Metasandstone	0.5	0.635	Disc	s, p
	6H-5, 142	45.62	Basalt	0.5	0.781	Rod	s, p
2	7H-4, 142	53.62	Phylite	0.3	0.414	Blade	
	8H-2, 86	59.56	Lithic wacke*	0.5	0.767	Sphere	w
	8H-3, 56	60.76	Metasandstone	0.6	0.735	Sphere	s
	8H-4, 23	61.93	Lithic wacke	0.5	0.884	Sphere	w, p, s
	8H-4, 46	62.16	Andesite	0.4	0.787	Sphere	s, p
	8H-4, 49	62.19	Quartz monzonite	0.4	0.594	Blade	
	8H-4, 75	62.45	Andesite	0.5	0.681	Disc	s, p
	8H-5, 23	63.43		0.3	0.551	Disc	
	8H-5, 142	64.62	Andesite	0.5	0.688	Disc	
	8H-6, 87	65.57	Diamict	0.4	0.593	Disc	
	8H-5, 45	63.65	Andesite	0.6	0.729	Disc	
	8H-3, 50	60.70	Metasandstone	0.5	0.688	Rod	p
	8H-6, 70	65.40	Quartz monzonite	0.2	0.599	Disc	
	8H-7, 12	66.32	Metasandstone	0.5	0.589	Disc	
	9H-6, 30	74.50	Granite	0.3	0.799	Sphere	
	10H-1, 29	76.49	Granodiorite	0.2	0.931	Sphere	
	10H-3, 125	80.45	Scoria	0.1	0.762	Sphere	
	10H-4, 38	81.08	Lithic wacke	0.5	0.658	Disc	
	10H-6, 110	84.80	Metasandstone	0.5	0.788	Sphere	

Table T1 (continued).

Unit	Core, section, interval (cm)	Depth (mbsf)	Lithology	Roundness	Sphericity	Shape	Surface texture
	11H-4, 48	90.68	Basalt	0.4	0.784	Rod	s
	11H-4, 73	90.93	Monzonite	0.3	0.773	Sphere	
	11H-5, 19	91.89	Metarhyolite	0.4	0.624	Blade	s, w
	11H-5, 61	92.31	Andesite	0.2	0.884	Sphere	
	12H-2, 21	96.91	Andesite	0.5	0.612	Disc	s
	12H-2, 22	96.92	Metarhyolite	0.5	0.689	Rod	p
	12H-2, 24	96.94	Rhyolite	0.2	0.577	Disc	s, C, p
	12H-2, 28	96.98	Metarhyolite	0.3	0.618	Blade	
	12H-2, 66	97.36	Diorite	0.4	0.815	Sphere	s
	12H-2, 77	97.47	Metarhyolite	0.4	0.493	Disc	
	12H-2, 89	97.59	Metarhyolite	0.2	0.59	Disc	
	12H-2, 103	97.73	Rhyolite	0.3	0.781	Sphere	w
	12H-4, 13	99.83	Basalt	0.5	0.724	Sphere	
	12H-5, 24	101.44	Rhyolite	0.3	0.684	Disc	
	12H-5, 120	102.40	Andesite	0.2	0.714	Rod	w
	12H-5, 121	102.41	Granite	0.5	0.688	Disc	
	12H-5, 147	102.67	Andesite	0.5	0.763	Rod	s, p
	13H-1, 107	105.77	Basalt	0.3	0.555	Disc	s
	13H-2, 140	107.60	Lithic wacke	0.2	0.7	Sphere	
	13H-4, 135	110.55	Andesite	0.5	0.625	Disc	
	13H-5, 19	110.89	Andesite	0.5	0.802	Sphere	
	13H-5, 59	111.29	Quartz monzonite	0.2	0.879	Sphere	
	13H-5, 65	111.35	Rhyolite	0.3	0.715	Sphere	
	13H-5, 82	111.52	Andesite	0.4	0.924	Sphere	
	13H-5, 82	111.52	Metaquartzite	0.6	0.687	Rod	
	14H-1, 24	114.44	Andesite	0.3	0.879	Sphere	
	14H-1, 52	114.72	Granite	0.2	0.738	Disc	
	14H-1, 75	114.95	Metasandstone	0.3	0.55	Disc	w
	14H-1, 145	115.65	Amphibolite	0.3	0.57	Rod	
	14H-3, 81	118.01	Granite	0.2	0.441	Disc	
	14H-4, 20	118.90	Granite	0.3	0.639	Disc	
	14H-4, 36	119.06	Lithic wacke	0.5	0.599	Disc	p
	14H-6, 87	122.57	Basalt	0.5	0.607	Rod	
	15H-2, 147	126.67	Rhyolite	0.4	0.665	Disc	
	15H-3, 39	127.09	Metarhyolite	0.4	0.712	Sphere	
	15H-5, 82	129.15	Latite	0.3	0.625	Disc	s, p
	15H-5, 83	129.16	Andesite	0.5	0.774	Sphere	p
	15H-6, 20	129.97	Quartz monzonite	0.5	0.803	Sphere	
3	17X-4, 91	148.11	Andesite	0.5	0.634	Blade	
	17X-6, 132	151.52	Trachyte	0.4	0.607	Disc	p
	18X-2, 36	152.36	Metarhyolite	0.3	0.597	Disc	p
	18X-6, 105	159.05	Andesite	0.4	0.769	Sphere	s, p
	19X-4, 50	165.10	Latite	0.3	0.609	Disc	s
	20X-4, 50	174.70	Rholite	0.4	0.745	Sphere	w, s
	20X-5, 71	176.41	Andesite	0.5	0.667	Rod	w, p
	20X-6, 142	178.62	Feldspathic wacke	0.5	0.637	Disc	
	21X-4, 16	183.96	Quartz monzonite	0.4	0.834	Sphere	w
	21X-4, 65	184.45	Lithic wacke	0.3	0.775	Sphere	
	22X-1, 132	190.22	Basalt	0.5	0.807	Sphere	s, p
	22X-2, 138	191.78	Andesite	0.2	0.525	Disc	s, p
	22X-3, 76	192.66	Trachyte	0.1	0.681	Disc	w
	22X-4, 23	193.63	Latite	0.5	0.703	Disc	
	22X-5, 49	195.39	Rhyolite	0.2	0.641	Disc	s

Notes: Sampled from Sites 1095, 1096, and 1101 of Leg 178 off the western margin of the Antarctic Peninsula. Surface texture symbols: w = weathering, s = striations, p = percussion marks. Sample numbers ending in letters indicate individual pebbles in samples having more than one pebble.